VIP Drug Delivery

DOI: 10.1002/anie.201107144

Well-Defined, Reversible Boronate Crosslinked Nanocarriers for Targeted Drug Delivery in Response to Acidic pH Values and *cis*-Diols**

Yuanpei Li, Wenwu Xiao, Kai Xiao, Lorenzo Berti, Juntao Luo, Harry P. Tseng, Gabriel Fung, and Kit S. Lam**

Stimuli-responsive nanoparticles are gaining considerable attention in the field of drug delivery because of their useful physicochemical changes in response to specific triggers, such as pH value,[1] temperature,[2] enzymes,[3] or redox conditions,[4] present in certain physiological or disease microenvironments of interest. Among these nanoparticles, stimuli-responsive cross-linked micelles (SCMs) represent a versatile nanocarrier system for tumor-targeting drug delivery.[2c,4,5] For instance, SCMs exhibit superior structural stability under physiological conditions compared to the non-cross-linked counterpart. As a result, these nanocarriers are able to better retain the encapsulated drug and minimize its premature release while circulating in the blood pool.[2c,4b,5b] The introduction of environmentally sensitive crosslinkers makes SCMs responsive to the local environment of the tumor (e.g. tumor extra-cellular pH 6.5–7.2, endosomal/lysosomal pH 4.5–6,[5b,6] and tumor reductive intra-cellular conditions[4–5]). In these instances, the payload drug is released almost exclusively in the cancerous tissue upon accumulation by the established enhanced permeation and retention (EPR) effect.[2c,4b,5b]

Remarkable progress in this field has led to the development of SCMs responsive to a single stimulus.[4b,5b] Various cleavable linkages have been introduced in SCMs, such as reducible disulfide bonds,[4b] pH cleavable,[6] or hydrolysable ester bonds.[2c] Currently, second-generation SCMs able to respond to multiple stimuli are being actively pursued as tools for accomplishing the multistage delivery of drugs to the complex in vivo microenvironment.[7] Boronic acids are able to bind diols reversibly forming boronate esters that exhibit fast dual responsiveness to external pH value and competing diols.[8] Based on this interaction, there has been increasing interest in using boronic acids as building blocks to design carbohydrate sensors,[9] nano-reactors,[10] drug delivery systems,[11] and self-healing materials.[12] Among diols, catechols are an excellent reactant for the formation of complexes with boronic acids, thanks to the favorable syn-peri-planar arrangement of the aromatic hydroxy groups combined with their electron-donating character.[8a,13] Herein, we present the first report on the synthesis of a novel class of dual-responsive boronate cross-linked micelles (BCM) for drug delivery based on the self-assembly and in situ complexation of boronic acid containing polymers and catechol containing polymers. We hypothesize that these BCMs will retain the encapsulated drug under physiological conditions, while releasing the payload quickly when triggered by the lower pH value of the tumor environment or when exposed to exogenous competing diols.

Additionally, we are also presenting a Förster resonance energy transfer (FRET) reporter system to evaluate the in vivo stability of these micelles. This characterization is usually difficult to accomplish in vivo due to the lack of suitable analytical techniques.

We have previously reported a novel class of micelles for efficient anticancer drug delivery based on linear polyethylene glycol (PEG) and dendritic cholic acids (CA) block copolymers (called telodendrimers).[4b,14] We have now improved the stability of these micelles by crosslinking with boronate esters at the core–shell interface. The crosslinking reactants (i.e. boronic acid and catechol) were introduced on the block copolymers through step-wise peptide chemistry by attachment to a hydrophilic linker and positioned onto adjacent sites of the telodendrimers (Scheme 1, Supporting Information Schemes S1, S2). The peptide chemistry employed provides a facile strategy to synthesize a number of well-defined telodendrimers bearing a defined number and derivative of boronic acids and catechols. Nitrophenylboronic acid (NBA) and phenylboronic acid (BA) were chosen as reactants to bind the catechol partners. The resulting boronate esters are known to be stable at physiological pH values[8a,15] even in the presence of most competing carbohydrates present in blood.[8a,b] The reaction of boronic acid with catechol on distinct telodendrimers in aqueous conditions takes place concomitantly to the self-assembly of the telodendrimers into micelles, resulting in boronate ester cross-linked micelles.

[*] Dr. Y. Li,[+] Dr. W. Xiao,[+] Dr. K. Xiao, Dr. L. Berti, H. P. Tseng, G. Fung, Prof. K. S. Lam
Department of Biochemistry and Molecular Medicine
UC Davis Cancer Center, University of California, Davis
2700 Stockton Blvd., Sacramento, CA 95817 (USA)
E-mail: kit.lam@ucdmc.ucdavis.edu
Prof. J. Luo
Department of Pharmacology, SUNY Upstate Cancer Research Institute, SUNY Upstate Medical University
Syracuse, NY 13210 (USA)
E-mail: luoj@upstate.edu
[+] These authors contributed equally to this work.

[**] This work was funded by NIH/NCI (R01CA115483 and R01CA140449), NIH/NIBIB (R01EB012569), and DoD BCRP Postdoctoral Award (W81XWH-10-1-0817).
Supporting information for this article is available on the WWW under http://dx.doi.org/10.1002/anie.201107144.

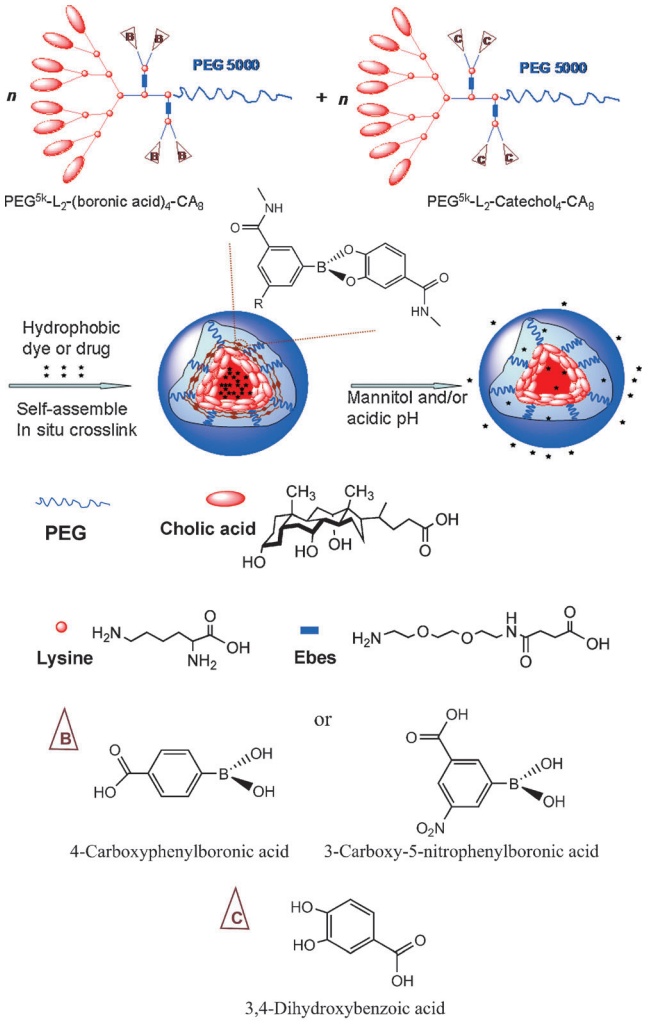

Scheme 1. Schematic representation of the telodendrimer pair [PEG^{5k}-(boronic acid or Catechol)$_4$-CA$_8$] and the resulting boronate crosslinked micelles (BCM) in response to mannitol and/or acidic pH values.

The synthetic schemes of a series of boronic acid and catechol-containing telodendrimers are shown in the Supporting information (Schemes S1–S3). A representative crosslinkable telodendrimer pair, PEG^{5k}-NBA$_4$-CA$_8$ (PEG^{5k} = PEG5000) and PEG^{5k}-catechol$_4$-CA$_8$ consist of, respectively, four nitrophenylboronic acids and four catechols, attached to the α- and ε-amino groups of pendant lysines positioned at adjacent sites between the linear PEG and dendritic octamer of cholic acids (Scheme S1–S3). The parent telodendrimer, PEG^{5k}-CA$_8$ was also synthesized[14b] to generate non-crosslinked micelles (NCM) for comparison. The structure of telodendrimers was confirmed by MALDI-TOF mass spectrometry, ^{1}H NMR spectroscopy, and a colorimetric assay based on the indicator of alizarin red S (ARS)[8a,16] (Supporting Information, Table S1, Figures S1–S3).

ARS is a catechol dye displaying dramatic changes in color upon binding to boronic acid (Figures S3, S4).[16] The introduction of electron withdrawing group onto the phenyl ring of boronic acid stabilizes the boronate form of the acid and lowers the pK_a value, which in turn favors boronate ester formation at a higher pH value of 7.4.[15] The nitrophenylboronic acids containing telodendrimer PEG^{5k}-NBA$_4$-CA$_8$ caused more significant color change of ARS (from burgundy to yellow) compared with the equal concentrations of phenylboronic acids containing telodendrimer PEG^{5k}-BA$_4$-CA$_8$, indicating the stronger binding of PEG^{5k}-NBA$_4$-CA$_8$ with ARS (Figure S4). ARS also exhibits dramatic changes in fluorescence intensity after forming esters with boronic acids (Scheme S4).[16] We observed that the fluorescence intensity of ARS at 580 nm increased significantly upon binding with PEG^{5k}-NBA$_4$-CA$_8$ and PEG^{5k}-BA$_4$-CA$_8$ (Figure S5). Next we proceeded to verify the formation of boronate crosslinking within BCMs. A series of BCMs composed of varying ratios of boronic acid- and catechol-containing telodendrimers was prepared by the solvent evaporation method.[4b,14] These micelles were then mixed with ARS (0.1 mM) and the fluorescence spectra were recorded. When the concentration of boronic acid containing telodendrimers within the micelles was fixed at 0.1 mM, the fluorescence of ARS was dramatically suppressed with increasing amounts of PEG^{5k}-Catechol$_4$-CA$_8$ (0 to 0.5 mM) (Figure 1 A, Supporting information Figure S6). These results

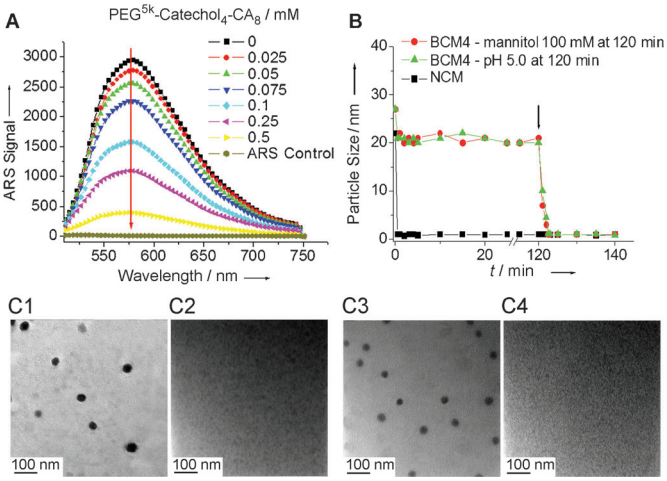

Figure 1. A) The fluorescent intensity of ARS (0.1 mM) upon mixing with micelles formed by PEG^{5k}-NBA$_4$-CA$_8$ (0.1 mM) with different ratios of PEG^{5k}-Catechol$_4$-CA$_8$ (0–0.5 mM) in PBS at pH 7.4. Excitation: 468 nm. B) Continuous dynamic light scattering measurements of NCM in SDS and BCM4 in SDS for 120 min, after which mannitol was added or the pH value of the solution was adjusted to 5.0 (see arrow). TEM images of BCM4 in PBS (C1), BCM4 in SDS for 120 min (C2), then after adjustment to pH 5.0 for 20 min (C3), or treatment with mannitol (100 mM) for 20 min (C4).

indicate the formation of catechol–boronate crosslinking esters as ARS was prevented from complexation with boronic acid containing telodendrimers.

A series of BCMs was formed using equal molar ratios of the boronic acid containing telodendrimers and catechol-containing telodendrimers and their physical properties are shown in Table 1. These micelles differed in the number of possible crosslinks per telodendrimer (2 vs 4) and the type of boronic acid used (BA vs NBA). We expect BCMs with

Table 1: Characterization of boronate crosslinked micelles and non-cross-linked micelles.

Micelle formulation	Telodendrimer pair	Size [nm][a]	CMC [$\mu g\,mL^{-1}$][b]	Stability in SDS[c]	PTX Content[d]
BCM1	PEG^{5k}-BA_2-CA_8, PEG^{5k}-Catechol$_2$-CA_8	23 ± 4	10.5	2 min	9.9%
BCM2	PEG^{5k}-NBA_2-CA_8, PEG^{5k}-Catechol$_2$-CA_8	26 ± 6	8.7	30 min	9.8%
BCM3	PEG^{5k}-BA_4-CA_8, PEG^{5k}-Catechol$_4$-CA_8	22 ± 3	7.4	5 min	9.8%
BCM4	PEG^{5k}-NBA_4-CA_8, PEG^{5k}-Catechol$_4$-CA_8	27 ± 5	4.2	Long term	9.9%
NCM	PEG^{5k}-CA_8	22 ± 6	50.1	<10 s	10.0%

[a] Measured by dynamic light scattering (DLS). [b] CMC = critical micelle concentration, measured by a fluorescent method by using pyrene as a probe. [c] The total period of time that the micelles retained their sizes in SDS, continuously measured by DLS every 10 s at pH 7.4. [d] PTX loading content of micelles (drug/polymer, w/w), in the presence of 20 $mg\,mL^{-1}$ of total telodendrimers and 2.0 $mg\,mL^{-1}$ PTX initial loading, measured by HPLC.

a higher number of crosslinks and NBA to be more stable. Boronate crosslinking dramatically reduced the critical micelle concentrations (CMC) as compared with NCM (Table 1). The particle sizes for BCMs were all in the range of 22–27 nm with narrow distribution (Table 1, Figure 1 B,C1, Figure S7), which is similar to the parent non-crosslinked PEG^{5k}-CA_8 micelles.

We investigated the interaction of the crosslinked micelles with plasma proteins to simulate potentially destabilizing conditions for in vivo applications. When exposed to 50% (v/v) human plasma for 24 h BCM4 still retained size uniformity and narrow distribution, with the main population at a particle size of 30 nm (Figure S-8E). In contrast, NCM showed significantly broader size and bimodal distribution with populations at 81 and 237 nm, indicating the formation of large aggregates (Figure S-8B). We investigated whether boronate crosslinking enhances micellar stability in severe micelle-disrupting conditions. Sodium dodecyl sulfate (SDS), a strong ionic detergent, has been reported to efficiently break down polymeric micelles.[17] Micelle solutions were exposed to an aqueous solution of SDS while continuously monitoring the particle size with dynamic light scattering. The rapid disappearance (<10 s) of the particle size signal for the NCM reflects the loss of integrity (Figures 1 B, S8 A, 8C). The BCM1, BCM2, and BCM3 retained their size in SDS for 2 min, 30 min, and 5 min, respectively (Table 1). Despite an initial decrease, the constant particle size was observed over 2 days for BCM4 treated under the same conditions, indicating that the crosslinked micelles self-assembled from the telodendrimer pair of PEG^{5k}-NBA_4-CA_8 and PEG^{5k}-Catechol$_4$-CA_8 remained intact (Figures 1 B, S8D, 8F and S9). BCM3 and BCM4, containing double the number of crosslinks (4 per telodendrimer) retained their structural integrity significantly longer in the presence of SDS, when compared to the corresponding BCM1 and BCM2 with only 2 crosslinks per telodendrimer. Since the pK_a value of NBA is lower than that of BA, BCM2, and BCM4 crosslinked by nitrophenylboronate esters were found to be more stable than the corresponding phenylboronate esters crosslinked micelles BCM1 and BCM3 in SDS at physiologic pH values We further investigated the response to pH value and diol for BCM4 in the presence of SDS. The particle size signal of BCM4 decreased suddenly (within 2 min) in SDS after 120 min incubation in pH 5.0, indicating that the micelle rapidly dissociated when a critical percentage of boronate bonds were hydrolyzed (Figures 1 B, S8G). We found that mannitol (containing three *cis*-diol pairs) could also efficiently cleave the crosslinking boronate bonds of the BCM4, as evidenced by the rapid reduction in particle size of BCM4 in the presence of SDS and excess of mannitol (100 mM) (Figure 1 A,B, Figure S8H). In contrast the size of BCM4 persisted in the presence of both SDS and 100 mM glucose (containing one *cis*-diol; Figure S8I).

TEM showed that the micellar structure of NCM was disrupted in SDS solution,[4b] and that the micellar structure of BCM4 was retained in SDS at pH 7.4 (Figure 1 C2) but was rapidly disrupted in SDS at pH 5.0 or in the presence of 100 mM mannitol (Figure 1 C3,C4).

We investigated the release profiles from the micelles by using paclitaxel (PTX) as a model drug. The loading content of PTX into NCM and BCMs was above 9.8% (w/w, drug/polymer) while the loading efficiency (percentage of drug encapsulated) for all micelles above 98%. PTX release from NCM was rapid with almost 30% of PTX released within the first 9 h independently from the pH value of the release medium or the presence of diols (Figure S10). PTX release from BCM3 crosslinked by phenylboronate was significantly slower than NCM but faster than BCM4 with nitrophenylboronate crosslinking at pH 7.4 (Figures S10A, S10B). PTX release from BCM3 was promoted when decreasing the pH of the medium from 7.4 to 6.5 while that of BCM4 was accelerated at pH 5.5 (Figure S10A). In the presence of glucose at its physiological level (2–10 mM) or even higher concentration (50 mM), PTX release from BCM3 and BCM4 was similar to that in the release media without glucose (Figure S10B). It was noted that PTX release was not sensitive to 10 mM mannitol but could be gradually facilitated as the concentration of mannitol increased up to the range of 50–100 mM (Figure S10B). This change could be attributed to the significantly higher affinity of mannitol with boronic acids than that of glucose at the same concentration in physiological conditions. Mannitol is a safe FDA approved drug for diuresis. A high blood level of mannitol (>50 mM) can be achieved clinically based on the recommended dose. Mannitol can thus be applied in vivo as an on-demand cleavage reagent by systemic intravenous injection to trigger drug release after the drug-loaded BCMs have accumulated in tumor sites. To simulate the in vivo situations, the PTX release from BCM4 was first incubated under physiological pH for a period of time (e.g. 5 h) and then was triggered with acidic pH and/or mannitol. As shown in Figure 2 A, the PTX release from BCM4 was significantly slower than that from

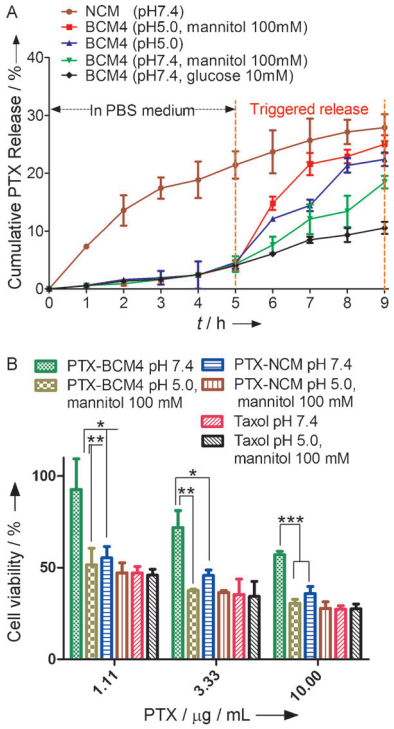

Figure 2. A) Paclitaxel (PTX) release profiles of BCM4 on treatment with diols (mannitol and glucose) and/or pH 5.0 after 5 h, and that of NCM. B) MTT assays showing the viability of SKOV-3 cells after 1 h incubation with Taxol, PTX-NCM, and PTX-BCM4 with or without treatment with 100 mM mannitol at pH 5.0, followed by three washes with PBS and additional 23 h incubation. *: $p<0.05$, **: $p<0.01$, ***: $p<0.001$.

NCMs at the initial 5 h. When 100 mM mannitol was added or the pH of the medium was adjusted to 5.0 at 5 h, there was a burst of drug release from the BCM4. Note that the PTX release can be further accelerated by the combination of 100 mM of mannitol and pH 5.0. This two-stage release strategy can be exploited so that premature drug release can be minimized during circulation in vivo followed by rapid drug release triggered by the acidic tumor microenvironment, or upon micelle exposure to the acidic compartments inside cancer cells, or by the additional administration of mannitol.

PEG^{5k}-NBA_4-CA_8, PEG^{5k}-$Catechol_4$-CA_8, and empty BCM4 showed no noticeable cytotoxicity to SKOV-3 ovarian cancer cells up to 1.0 mg mL^{-1} (Figure S11). Confocal laser scanning microscopic images showed that BCM4 loaded with a hydrophobic near infrared dye (DiD) were taken up by SKOV-3 ovarian cancer cells and mainly localized in the cytoplasmic region after 1 h incubation (Figure S12). The in vitro anticancer activity of PTX loaded non-crosslinked micelles (PTX-NCM) and PTX-loaded BCM4 (PTX-BCM4) was evaluated on SKOV-3 ovarian cancer cells for 1 h incubation followed by PBS wash and 23 h further incubation. PTX-NCM showed in vitro antitumor effects against SKOV-3 cells comparable to Taxol (free drug of paclitaxel; Figure 2B). PTX-BCM4 was found to be considerably less cytotoxic than Taxol and PTX-NCM at equal dose levels. This reflects the fact that less PTX exposed to cells caused by slower drug release from BCM4 within the cell culture media at pH 7.4 in the presence of 5.5 mM glucose (Figure 2B). There were minimal changes in the toxicity profile of PTX-NCM and free drug triggered with acidic pH and mannitol. In contrast, PTX-BCM4 showed significantly enhanced cancer cell inhibition at pH 5.0 in the presence of mannitol (100 mM; Figure 2B). The enhanced stability of BCM4 means it is expected to deliver higher concentrations of PTX to tumor site than NCM for in vivo applications. Subsequent release on-demand should result in better antitumor effects.

We then developed a FRET system to evaluate the in vivo stability of the crosslinked micelles. FRET is a powerful technique to probe the molecular proximity of a fluorescent donor–acceptor pair[18] and for this reason FRET has been widely applied in the investigation of a variety of biological events.[18] Very recently, few reports utilized FRET to probe the stability and drug-release profile of non-crosslinked micelles.[19]

We constructed the FRET reporter system by using a green dye DiO (donor) and a red-orange dye rhodamine B (acceptor) as a FRET pair (Figure 3A, Figure S13). DiO was encapsulated in the core of micelles as the hydrophobic drug surrogate to track the payloads. Rhodamine B was covalently conjugated to the telodendrimers to track the nanocarriers. When the 20 nm non-crosslinked FRET micelle (FRET-NCM) was intact, the proximity between DiO and rhodamine B was within the FRET range allowing efficient energy transfer from DiO to rhodamine B upon excitation of DiO at 480 nm (Figures 3C, S13). The FRET ratio ($I_{\text{rhodamine B}}/(I_{\text{rhodamine B}}+I_{\text{DiO}})$) was measured to be 80%, where $I_{\text{rhodamine B}}$ and I_{DiO} are the fluorescence intensity of rhodamine B at 580 nm and DiO at 530 nm, respectively, in PBS. Upon FRET-NCM dissociation, the FRET ratio was significantly reduced to 21% as result of the separation between DiO and rhodamine B (Figure 3B,C). A FRET signal was also detected from boronate crosslinked FRET micelles (FRET-BCM4, particle size: 21 nm) with an observed FRET ratio of 89% in PBS (Figure 3D). Significant DiO emission at 530 nm was observed along with dramatic reduction of rhodamine B fluorescence when FRET-BCM4 was diluted 20 times with DMSO, indicating a loss of FRET signal due to the solvation of DiO when the micelle was dissolved. Upon excitation at 480 nm, the rhodamine B signal of NCM and BCM4 labeled with rhodamine B alone was negligible in comparison with the corresponding FRET micelles (Figure S13C, S13D). Therefore, by monitoring the dynamic change of FRET ratio, we were able to monitor the stability of the micelles in real time.[4b,19a] FRET micelles were injected into nude mice at the tail vein and the blood was collected at different times to investigate the micelle in vivo stability by monitoring FRET efficiency. The FRET ratio of FRET-NCM decreased rapidly to 46% within 1 min post-injection and dropped to 21% after 24 min (Figure 3E, Figure S14). One possible reason is the dissociation of NCM upon extreme dilution in blood stream as the estimated concentration of micelles in blood (100 μg mL^{-1}) was close to their CMC (50.1 μg mL^{-1}, Table 1).[20] Moreover, blood flow with a strong shear stress could mix the micelles thoroughly with blood proteins and lipoprotein nanoparticles (e.g. LDL, HDL, VLDL), leading to a fast release of core-loaded DiO dye from the circulating

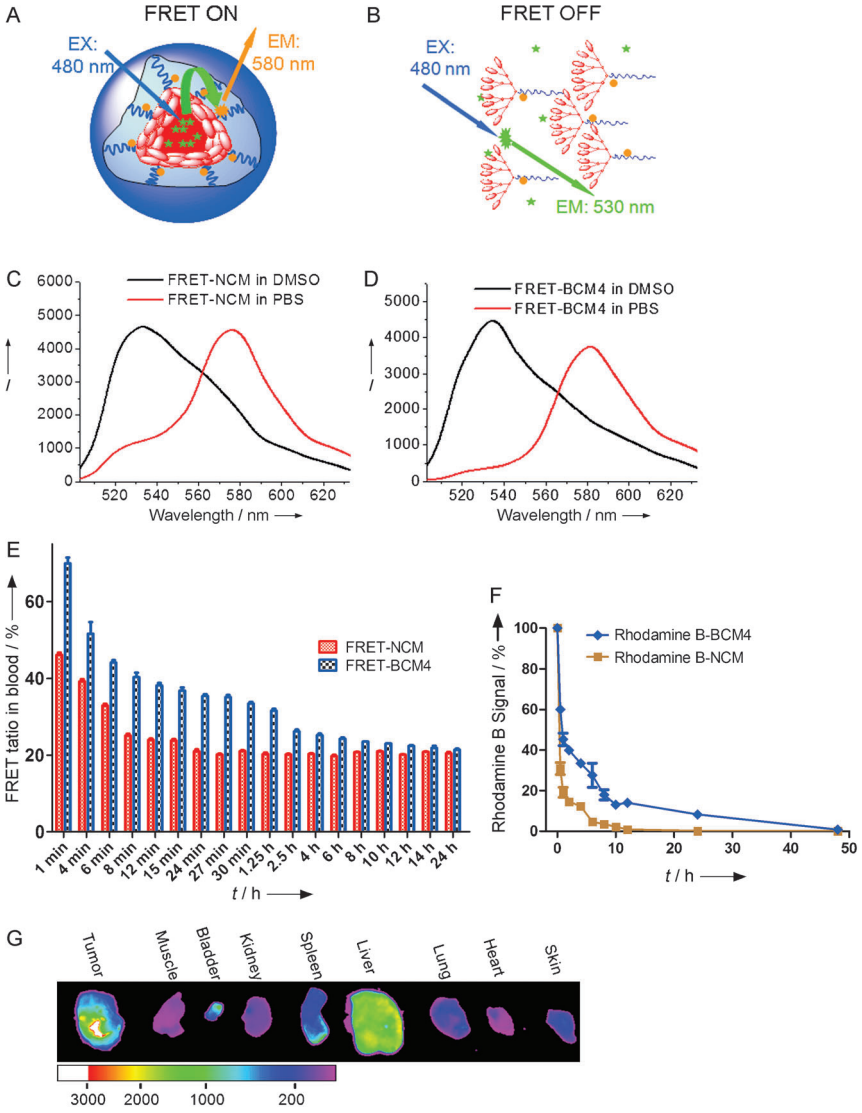

Figure 3. Schematic illustration of FRET-NCM in PBS (A) and in DMSO (B) at pH 7.4. C) Fluorescence emission spectra of FRET-NCM in PBS (red line) and in DMSO (black line) with 480 nm excitation. D) Emission spectra of FRET-BCM4 in PBS (red line) and DMSO (black line) with 480 nm excitation. E) The FRET ratio in blood of nude mice ($n=3$) over time after intravenous injection of 100 μL FRET-NCM and FRET-BCM4 (2.0 mg mL^{-1}). Excitation: 480 nm. F) The fluorescence signal changes of rhodamine B conjugated NCM and BCM4 in the blood collected at different times after intravenous injection in the nude mice ($n=3$). Excitation: 540 nm. G) Ex vivo near infrared fluorescence (NIRF) images of SKOV-3 xenograft after intravenous injection of BCM4 co-loaded with PTX and DiD.

micelles.[19a] In contrast, the FRET ratio of FRET-BCM4 decreased much more slowly than that of FRET-NCM at the same micelle concentration (Figure 3E, Figure S14), indicating the boronate crosslinking greatly enhances the in vivo stability of the micelles, therefore, will decrease premature payload release.

Rhodamine B labeled NCM and BCM4 were used to study the in vivo blood elimination kinetics of the micelles (Figure S15). After intravenous injection into mice, the rhodamine B signal of NCM was rapidly eliminated from blood circulation and fell into the background level within 10 h post injection (Figure 3F). Rhodamine B signal of BCM4 in blood was six-times higher than that of NCM at 10 h post injection and the signal was sustained for more than 24 h. The profiles of elimination kinetics indicated that the crosslinked micelles have longer blood circulation time than the non-crosslinked micelles. We further demonstrated DiD and PTX co-loaded BCM4 are able to preferentially accumulate in SKOV-3 ovarian tumor (Figure S16). Ex vivo imaging at 32 h post injection confirmed the preferential uptake of BCM4 in tumor compared to normal organs (Figure 3G). This is due to the prolonged in vivo circulation time of the micelles and the size-mediated EPR effect.

In summary, we reported the design and synthesis of a novel class of dual pH value and diol-responsive crosslinked micelles formed by well-defined telodendrimers containing boronic acid and catechol, respectively. By tuning the pK_a and numbers of boronic acids and catechols in the telodendrimers, we have optimized the stability of the resulting boronate crosslinked micelles as well as their stimuli-response to *cis*-diols and acidic pH values. The release of PTX from the boronate crosslinked micelles was significantly slower than that from non-crosslinked micelles but can be accelerated by the acidic pH values and/or mannitol. We developed a highly efficient FRET system and further demonstrated that BCMs exhibited enhanced in vivo stability. This novel nanocarrier shows great promise for drug delivery with minimal premature drug release at physiological glucose level (2–10 mM) and physiological pH values (pH 7.4) in blood circulation but can be activated to release drug on demand at the acidic tumor microenvironment or in the acidic cellular compartments upon uptake in target tumor cells, and/or by the additional intravenous administration of mannitol as an on-demand triggering agent.

Received: October 9, 2011
Published online: January 17, 2012

Keywords: boronate · controlled release · FRET · micelles · nanocarriers

[1] a) K. Zhou, Y. Wang, X. Huang, K. Luby-Phelps, B. D. Sumer, J. Gao, *Angew. Chem.* **2011**, *123*, 6233–6238; *Angew. Chem. Int. Ed.* **2011**, *50*, 6109–6114; b) Y. Lee, T. Ishii, H. Cabral, H. J. Kim, J. H. Seo, N. Nishiyama, H. Oshima, K. Osada, K. Kataoka, *Angew. Chem.* **2009**, *121*, 5413–5416; *Angew. Chem. Int. Ed.*

2009, *48*, 5309 – 5312; c) J. Z. Du, T. M. Sun, W. J. Song, J. Wu, J. Wang, *Angew. Chem.* **2010**, *122*, 3703 – 3708; *Angew. Chem. Int. Ed.* **2010**, *49*, 3621 – 3626; d) P. Xu, E. A. Van Kirk, Y. Zhan, W. J. Murdoch, M. Radosz, Y. Shen, *Angew. Chem.* **2007**, *119*, 5087 – 5090; *Angew. Chem. Int. Ed.* **2007**, *46*, 4999 – 5002; e) E. S. Lee, K. Na, Y. H. Bae, *Nano Lett.* **2005**, *5*, 325 – 329.

[2] a) Y. Li, S. Pan, W. Zhang, Z. Du, *Nanotechnology* **2009**, *20*, 065104; b) E. L. Chaikof, W. Kim, J. Thevenot, E. Ibarboure, S. Lecommandoux, *Angew. Chem.* **2010**, *122*, 4353 – 4356; *Angew. Chem. Int. Ed.* **2010**, *49*, 4257 – 4260; c) C. J. Rijcken, C. J. Snel, R. M. Schiffelers, C. F. van Nostrum, W. E. Hennink, *Biomaterials* **2007**, *28*, 5581 – 5593.

[3] a) R. V. Ulijn, P. D. Thornton, R. J. Mart, *Adv. Mater.* **2007**, *19*, 1252 – 1256; b) B. Law, R. Weissleder, C. H. Tung, *Bioconjugate Chem.* **2007**, *18*, 1701 – 1704.

[4] a) F. H. Meng, Y. L. Li, L. Zhu, Z. Z. Liu, R. Cheng, J. H. Cui, S. J. Ji, Z. Y. Zhong, *Angew. Chem.* **2009**, *121*, 10098 – 10102; *Angew. Chem. Int. Ed.* **2009**, *48*, 9914 – 9918; b) Y. Li, K. Xiao, J. Luo, W. Xiao, J. S. Lee, A. M. Gonik, J. Kato, T. A. Dong, K. S. Lam, *Biomaterials* **2011**, *32*, 6633 – 6645.

[5] a) S. C. Lee, A. N. Koo, H. J. Lee, S. E. Kim, J. H. Chang, C. Park, C. Kim, J. H. Park, *Chem. Commun.* **2008**, 6570 – 6572; b) W. E. Hennink, M. Talelli, M. Iman, A. K. Varkouhi, C. J. F. Rijcken, R. M. Schiffelers, T. Etrych, K. Ulbrich, C. F. van Nostrum, T. Lammers, G. Storm, *Biomaterials* **2010**, *31*, 7797 – 7804.

[6] M. M. Q. Xing, C. H. Lu, W. Zhong, *Nanomed-Nanotechnol* **2011**, *7*, 80 – 87.

[7] a) C. Wei, J. Guo, C. Wang, *Macromol. Rapid Commun.* **2011**, *32*, 451 – 455; b) N. Ma, Y. Li, H. Xu, Z. Wang, X. Zhang, *J. Am. Chem. Soc.* **2010**, *132*, 442 – 443; c) J. Dai, S. Lin, D. Cheng, S. Zou, X. Shuai, *Angew. Chem.* **2011**, *123*, 9576 – 9580; *Angew. Chem. Int. Ed.* **2011**, *50*, 9404 – 9408.

[8] a) G. Springsteen, B. H. Wang, *Tetrahedron* **2002**, *58*, 5291 – 5300; b) L. Zhu, S. H. Shabbir, M. Gray, V. M. Lynch, S. Sorey, E. V. Anslyn, *J. Am. Chem. Soc.* **2006**, *128*, 1222 – 1232; c) Y. Qin, V. Sukul, D. Pagakos, C. Z. Cui, F. Jakle, *Macromolecules* **2005**, *38*, 8987 – 8990; d) B. S. Sumerlin, D. Roy, J. N. Cambre, *Chem. Commun.* **2008**, 2477 – 2479.

[9] a) S. Li, E. N. Davis, J. Anderson, Q. Lin, Q. Wang, *Biomacromolecules* **2009**, *10*, 113 – 118; b) C. Cannizzo, S. Amigoni-Gerbier, C. Larpent, *Polymer* **2005**, *46*, 1269 – 1276; c) J. C. M. van Hest, K. T. Kim, J. J. L. M. Cornelissen, R. J. M. Nolte, *J. Am. Chem. Soc.* **2009**, *131*, 13908 – 13909.

[10] J. C. M. van Hest, K. T. Kim, J. J. L. M. Cornelissen, R. J. M. Nolte, *Adv. Mater.* **2009**, *21*, 2787 – 2791.

[11] a) W. Wu, L. Z. Zhang, Y. Lin, J. J. Wang, W. Yao, X. Q. Jiang, *Macromol. Rapid Commun.* **2011**, *32*, 534 – 539; b) L. Q. Shi, B. L. Wang, R. J. Ma, G. Liu, Y. Li, X. J. Liu, Y. L. An, *Langmuir* **2009**, *25*, 12522 – 12528; c) Y. Zhao, B. G. Trewyn, Slowing II, V. S. Lin, *J. Am. Chem. Soc.* **2009**, *131*, 8398 – 8400.

[12] L. He, D. E. Fullenkamp, J. G. Rivera, P. B. Messersmith, *Chem. Commun.* **2011**, *47*, 7497 – 7499.

[13] F. Marken, Y. J. Huang, Y. B. Jiang, J. S. Fossey, T. D. James, *J. Mater. Chem.* **2010**, *20*, 8305 – 8310.

[14] a) J. Luo, K. Xiao, Y. Li, J. S. Lee, L. Shi, Y. H. Tan, L. Xing, R. Holland Cheng, G. Y. Liu, K. S. Lam, *Bioconjugate Chem.* **2010**, *21*, 1216 – 1224; b) K. Xiao, J. Luo, W. L. Fowler, Y. Li, J. S. Lee, L. Xing, R. H. Cheng, L. Wang, K. S. Lam, *Biomaterials* **2009**, *30*, 6006 – 6016; c) Y. Li, K. Xiao, J. Luo, J. Lee, S. Pan, K. S. Lam, *J. Controlled Release* **2010**, *144*, 314 – 323; d) K. Xiao, Y. Li, J. Luo, J. S. Lee, W. Xiao, A. M. Gonik, R. G. Agarwal, K. S. Lam, *Biomaterials* **2011**, *32*, 3435 – 3446.

[15] H. R. Mulla, N. J. Agard, A. Basu, *Bioorg. Med. Chem. Lett.* **2004**, *14*, 25 – 27.

[16] G. Springsteen, B. Wang, *Chem. Commun.* **2001**, 1608 – 1609.

[17] A. N. Koo, H. J. Lee, S. E. Kim, J. H. Chang, C. Park, C. Kim, J. H. Park, S. C. Lee, *Chem. Commun.* **2008**, 6570 – 6572.

[18] a) E. A. Jares-Erijman, T. M. Jovin, *Nat. Biotechnol.* **2003**, *21*, 1387 – 1395; b) R. B. Sekar, A. Periasamy, *J. Cell Biol.* **2003**, *160*, 629 – 633; c) K. E. Sapsford, L. Berti, I. L. Medintz, *Angew. Chem.* **2006**, *118*, 4676 – 4704; *Angew. Chem. Int. Ed.* **2006**, *45*, 4562 – 4589.

[19] a) H. Chen, S. Kim, W. He, H. Wang, P. S. Low, K. Park, J. X. Cheng, *Langmuir* **2008**, *24*, 5213 – 5217; b) K. J. Chen, Y. L. Chiu, Y. M. Chen, Y. C. Ho, H. W. Sung, *Biomaterials* **2011**, *32*, 2586 – 2592; c) K. Park, H. T. Chen, S. W. Kim, L. Li, S. Y. Wang, J. X. Cheng, *Proc. Natl. Acad. Sci. USA* **2008**, *105*, 6596 – 6601.

[20] J. X. Cheng, S. Kim, Y. Z. Shi, J. Y. Kim, K. Park, *Expert Opin. Drug Delivery* **2010**, *7*, 49 – 62.

